X International Conference on Computational Methods in Marine Engineering
MARINE 2023
J. Garcia-Espinosa, L. González, J.E. Gutiérrez & B. Serván-Camas (Editors)

Numerical Study of the Effect of Inclined Columns on the Performance of Floating Offshore Wind Turbine Platform

Yinjie Xue[1], Xiaoming Zhang[2], Decheng Wan[1*]

[1] Computational Marine Hydrodynamics Lab (CMHL), School of Naval Architecture, Ocean and Civil Engineering, Shanghai Jiao Tong University, Shanghai, China
[2] Zhongnan Engineering Corporation Limited, Changsha, China

[*] Corresponding author: dcwan@sjtu.edu.cn

ABSTRACT

With the gradual development of the international wind power industry and deep-sea energy, the larger floating offshore wind turbine (FOWT) has become an attractive issue. In order to ensure the rotor normal operation, larger and stronger structure design are used which greatly increase the quality and capital of the platform. In this study, the inclined angle at 10 degrees and 20 degrees for OC4 FOWT platform are modeled. The structural properties such as light mass, ballast mass, center of mass and moment inertia are provided detailly. Based on the computational fluid dynamic technique, the hydrodynamics of these modification platform was tested compared with original platform. Under the same draft condition, it is found that the inclined angle could reduce the amplitude of pitch motion 13.57 % and 15.57 % respectively, mainly because of improvement of the moment inertia which is beneficial for platform stability.

Keywords: floating offshore wind turbine platform; inclined column; hydrodynamic response; computational fluid dynamics;

NOMENCLATURE

A	Cross-sectional area of the mooring lines [m^2]
D	Hydrodynamic forces of mooring lines in normal direction [N]
F	Hydrodynamic forces of mooring lines in tangential direction [N]
f_ε	Surface tension term
$\boldsymbol{g}$	Gravitational acceleration vector [m s^{-2}, m s^{-2}, m s^{-2}]
$\boldsymbol{k}$	Wave number vector
L_s	Length of sponger layer [m]
p_d	Dynamic pressure [Pa]
T	Mooring tension [N]
$\boldsymbol{U}$	Velocity of flow filed vector [m s^{-1},m s^{-1},m s^{-1}]
$\Delta z'$	Vertical distance between two ending nodes of mooring segments [m]
α_s	Custom viscosity parameter
α_v	Volume fraction
β	Wave direction angle[°]
δ	Wave phase
μ_{eff}	Effective dynamic viscosity coefficient of the water [N s m^{-2}]
ρ	Fluid density [kg m^{-3}]
ω_i	Submerged weight of mooring lines per meter [kg m^{-1}]
CFD	Computational Fluid Dynamics
CoM	Center of Mass
DOF	Degree of Freedom
NREL	National Renewable Energy Laboratory
PEM	Piecewise Extrapolating Method

PISO Pressure-Implicit with Splitting of Operators
RAO Response Amplitude Operator
SIMPLE Semi-Implicit-Method for Pressure Linked Equations

1. INTRODUCTION

With the rapid development of new energy, the offshore wind power projects have become a focus. According to the Global Wind Energy Council's report, the total offshore capacity has become to 57 GW (GWEC, 2022). At present, the lower production capacity of inshore fixed electric filed limited by wind speed promotes the development of floating offshore wind power (Bagbanci *et al.*, 2012). While, with the trend of large-scale blades and platforms, complex and harsh sea conditions put forward requirements for floating platform structures (Xu *et al.*, 2022), and the cost of a single offshore floating wind power is extremely high. Therefore, it is necessary to do more research on the optimization design and parameterization analysis of the floating offshore wind turbine (FOWT) platform.

Early studies, such as Sclavounos *et al.* (2008), they used the simplified equations to parameterize the motion response of the platforms with different draft and diameter. The Pareto fronts for the nacelle acceleration, mooring tension, and displacement were carried out from the calculation results. They found that the optimization results are generally best performed on the narrow deep drafted spar or shallow barge ballasted with concrete. Brommundt *et al.* (2012) optimized the design of mooring cables, exploring the optimal layout and minimum mooring costs in specific environmental locations. A multi-objective method for FOWT platform was proposed by Karimi *et al.* (2017), defining the main body, cross-bracing or other structures by nine variable parameters. Based on the frequency domain analysis, a Pareto front was constructed and the multi-objective genetic algorithm was used to optimize the cost of installation and power of wind turbine.

The OC4 is a semi-submersible floating platform designed to support NREL 5MW wind turbine, which was proposed by Robertson *et al.* (2014). This model has gradually become a validation model for experimental research and numerical simulation of floating offshore wind turbine (Cheng *et al.*, 2019; Coulling *et al.*, 2013; Tran and Kim, 2015; Xu *et al.*, 2023). Ferri *et al.* (2020) expanded the OC4 platform to support a 10MW wind turbine. And the diameter of outer column and their radial distance are optimized. Aiming to reduce the response amplitude operator (RAO) peak, there are 32 models coupled by both two parameters are calculated under white noise wave conditions based on frequency domain analysis. They found that the RAO motion response doesn't exhibit a linear relationship with the changes in those two parameters, which means there is an optimal solution. The model after optimization could reduce the RAO peak of heave and pitch 54% and 50% respectively. Later, their team (Ferri *et al.*, 2022) used genetic algorithms to optimize the radius, spacing, and draft of the modified 10MW platform. The multi-segmented mooring lines are adopted by Liu *et al.* (2019), and the inclined columns with 15° and 30° inclined angle are modeled. The motion response and mooring tension under different load conditions are calculated under multiple regular and irregular wave conditions by their inhouse code based on potential theory. Comparing with the original OC4 model, the angle of inclined column can effectively reduce heave and pitch motion in the high frequency wave. Zhang *et al.* (2022) combined the structural characteristic of OC3 spar platform and OC4 semi-submersible platform to design a new platform with inclined side columns. The results show that the inclined columns could significantly optimize the hydrodynamic performance due to enlarge the moment of inertia, while without increasing the stress.

From previous research, although the optimized designs of OC4 platform have been done more, most of them use potential flow method for rapid research. Besides, there are less suggestions for design details about steel mass or ballast water provided. In this paper, the OC4 platform with 10° and 20° inclined angle of offset columns are designed and modeled, providing the light weight of platform and ballast properties etc. for each model. The motion hydrodynamic response of the modified platforms and original platform is simulated by inhouse code naoe-FOAM-SJTU solver based on computational fluids dynamic (CFD) method. The naoe-FOAM-SJTU is developed on the basis of open source software OpenFOAM (Wang *et al.*, 2019). In section

2, the numerical theory and the coupled of mooring calculation and 6DOF analysis of naoe-FOAM-SJTU are introduced. In section 3, the properties of original OC4 model and inclined models are provide. Besides, the mesh grid and simulation domain are also introduced in this section. The section 5 mainly talks about the calculation results of different models. Besides, the load condition and validation for wave generation are shown in this section.

2. NUMERICAL METHOD

2.1 Governing Equations

In present study, the simulation technique is based on CFD method by OpenFOAM source code. Try to calculate the fluid information, the Navier Stokes (NS) equation must be solved, which is also called governing equation of fluid mechanics. There are two equations continuity and momentum equation included in incompressible NS equation:

$$\nabla \cdot \boldsymbol{U} = 0 \tag{1}$$

$$\frac{\partial \rho \boldsymbol{U}}{\partial \mathrm{t}} + \nabla \cdot (\rho \boldsymbol{U}\boldsymbol{U}) = -\nabla p_d - \boldsymbol{g} \cdot \boldsymbol{x} \nabla \rho + \nabla \cdot \left(\mu_{eff} \nabla \boldsymbol{U}\right) + f_\varepsilon \tag{2}$$

where, $\boldsymbol{U}$ represents the velocity of flow filed; ρ is the density of the fluid (water), equal to 1025 kg/m^3 in this paper; g is the acceleration vector of gravity, equal to 9.80665 m/s^2; The dynamic pressure p_d is equal to the total pressure minus the hydrostatic pressure, as: $p_d = p - \rho \boldsymbol{g} \cdot \boldsymbol{x}$. μ_{eff} is the effective dynamic viscosity coefficient of the water and f_ε is the surface tension term. Direct solution of NS equations requires an extremely grid distribution, so various turbulence models are usually used to analyze the problem of fluid turbulence, like *k-ε*, *k-ω*, LES etc.

2.2 Volume of Fluid (VOF) Method

The VOF method is a two-phase flow method which is used to capture the free surface proposed by Hirt and Nichols (1981). In this method, each cell is defined by a volume fraction variable, which represents the volume ratio of one fluid in this cell. Normally, the volume fraction α_v equal to zero represents the air phase, and equal to 1 represents the water phase.

$$\begin{cases} \alpha_v = 0 & \text{air} \\ 0 < \alpha_v < 1 & \text{freesurface} \\ \alpha_v = 1 & \text{water} \end{cases} \tag{3}$$

The transport equation of VOF can be described as:

$$\frac{\partial \alpha_v}{\partial t} + \nabla \cdot (\alpha_v \boldsymbol{U}) = 0 \tag{4}$$

For the two-phase flow problems, the density of fluid ρ and dynamic viscosity μ can be described as:

$$\begin{cases} \rho = \alpha_v \, \rho_l + (1 - \alpha_v)\rho_g \\ \mu = \alpha_v \, \mu_l + (1 - \alpha_v)\mu_g \end{cases} \tag{5}$$

where, the subscript *l* and *g* represents the liquid (water) and gas (air) respectively.

2.3 Wave Generation and Absorption Module

In naoe-FOAM-SJTU solver, many types of wave generation are introduced such as regular wave, irregular wave, white noise wave spectrum, focused wave etc. The stokes first deep water is applied to generate a regular wave in this paper, and its wave elevation and velocities are calculated using the following equations:

$$\eta = a\cos\left(\boldsymbol{k}\cdot\boldsymbol{x} - \omega t + \delta\right) \tag{7}$$

$$\begin{cases} u = a\omega e^{kz}\cos\left(\boldsymbol{k}\cdot\boldsymbol{x} - \omega t + \delta\right) \\ v = a\omega e^{kz}\cos\beta\cos(\boldsymbol{k}\cdot\boldsymbol{x} - \omega t + \delta) \\ w = a\omega e^{kz}\sin\beta\sin(\boldsymbol{k}\cdot\boldsymbol{x} - \omega t + \delta) \end{cases} \tag{8}$$

where, β is wave direction defined as the angle between the wave and the x-coordinate of the earth-fixed coordinate system; $\boldsymbol{k}$ is the wave number considering direction; δ represents the wave phase, equal to 0 in this paper.

The wave reflection of waves on the outlet boundary would cause computational oscillations, which make it necessary to add a wave damping zone at the end of tank to ensure the accuracy of the calculation results. By adding a sponge layer at the exit in damping zone, the NS equation is modified in the form of the source term f_s.

$$f_s(x) = \begin{cases} -\rho\alpha_s\left(\dfrac{\boldsymbol{x}-\boldsymbol{x}_s}{L_s}\right)^2\boldsymbol{U} & inside\ sponge\ layer \\ 0 & outside\ sponge\ layer \end{cases} \tag{9}$$

where, α_s is custom viscosity parameter, $\alpha_s = 10$ in this paper; L_s is the length of sponge layer, and the $\boldsymbol{x}_s$ is location of damping zone start point in the wave tank.

2.4 Mooring System

In general, the time-domain analysis of offshore floating structures is carried out for 6DOF motion. Since floating structures do not have restoring forces in *x*-axial *y*-axial and rotating around the z-axial three directions, mooring systems must be considered to limit platform motion. In naoe-FOAM-SJTU, a quasi-static model method which called piecewise extrapolating method (PEM) is developed to calculate the mooring forces (Cheng, 2019). In this method, an entire mooring cable is divided into many chain segments, and the calculation result will be extrapolated from the previous segment to the next segment until to the end as Fig. xxx and following equations:

$$\begin{cases} T_{xi+1} - T_{xi} - F_i\,\mathrm{d}s\cos\varphi_{i+1} - D_i\,\mathrm{d}s\sin\varphi_{i+1} = \rho g A\Delta z'\cos\varphi_{i+1} \\ T_{zi+1} - T_{zi} - F_i\,\mathrm{d}s\sin\varphi_{i+1} - D_i\,\mathrm{d}s\cos\varphi_{i+1} - \omega_i\mathrm{d}l = \rho g A\Delta z'\sin\varphi_{i+1} \end{cases} \tag{10}$$

where, T_x and T_z represent the components of the mooring tension in the horizontal and vertical directions respectively; D and F represent the components of hydrodynamic forces in normal and tangential directions; $\mathrm{d}l$ and $\mathrm{d}s$ is the length of cable before and after stretching respectively; ω_i is the submerged weight of lines per meter; A is the equivalent cross-sectional area of the mooring line; $\Delta z'$ is the vertical distance between two ending nodes of the segments.

2.5 Hydrodynamic Coupling Calculation

The code our team developed naoe-FOAM-SJTU has coupled the wave generation and absorption and mooring system above mentioned to solve 6DOF calculation of floating structures, like Fig. 2. In addition, there are two coordinates system set up the predict the motions response. In each time step, the motions are calculated in the

body-fixed system and the forces are calculated in earth-fixed coordinate system. Both of them transfer their information by through transformation matrices.

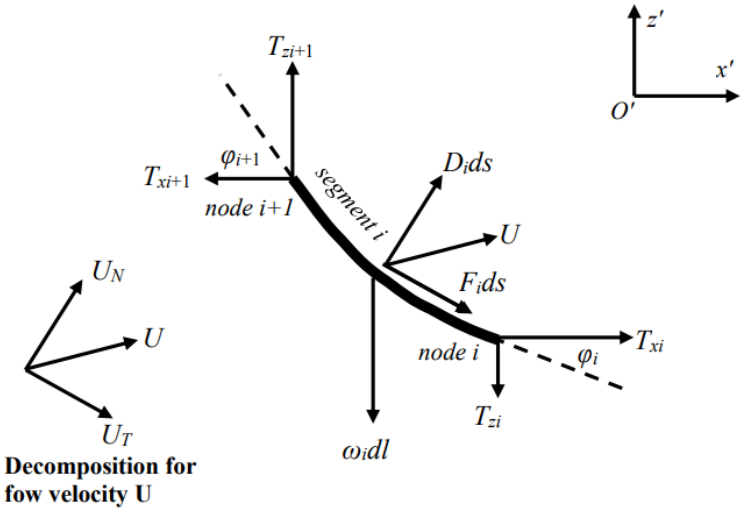

Figure 1. Analysis of mooring forces in cable segment.

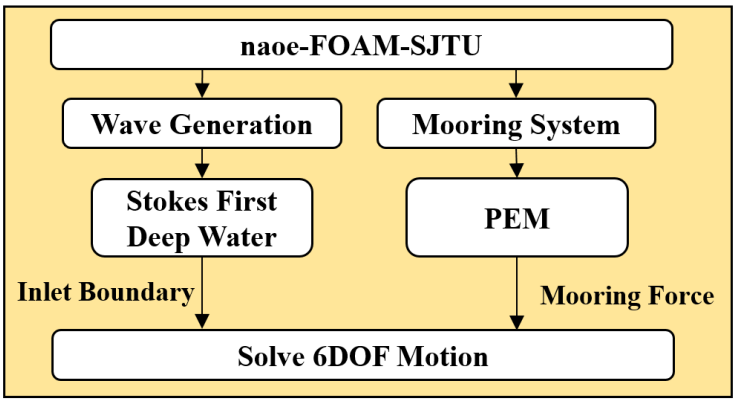

Figure 2. The coupled of analysis module in naoe-FOAM-SJTU

2.6 Simulation Method and Discrete Formats

All the simulations are employed PIMPLE algorithm which is merged with PISO and SIMPLE solution algorithm in OpenFOAM. In the inner lop, the PISO algorithm is used to calculate the pressure correction with limited iterations. While in the outer lop, the SIMPLE algorithm regards each time as a steady flow, and the absolute tolerance and number of iterations are considered as convergence criteria. Therefore, a greater stability of calculation can also be guaranteed using larger time step. Besides, in this paper, the solution method for velocity U is chosen as a second-order scheme name Gauss linaerUpwind, and the time precision discrete format is chosen as CrankNicolson which is a second-order in OpenFOAM.

3. MODELING MODIFICATION AND SIMULATION DOMAIN SETTING

3.1 Original Parameters of OC4

Multiple physical parameters such as geometric mass, moment of inertia, light weight information, ballast water and the steel plate thickness of each structural components etc. are provided in detail in Robertson's report (Robertson et al., 2014).

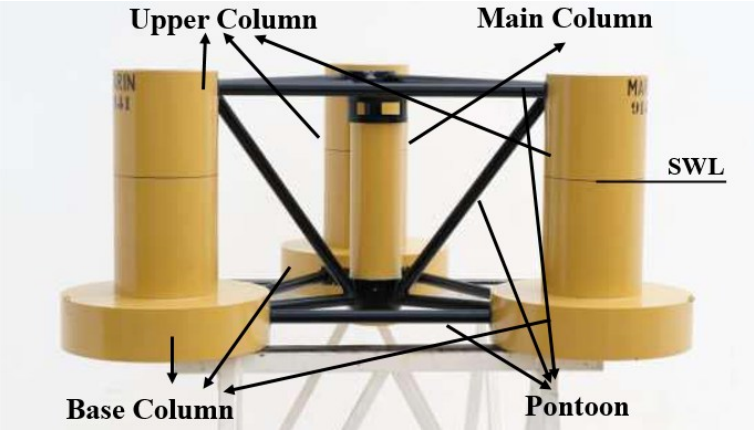

Figure 3. OC4 semi-submersible floating platform model (Robertson et al., 2014).

The total platform can be divided into four components, main column, upper column, base column and pontoon, such as Fig. 3. More platform geometry parameters are listed in Tabs.1a. The research of the hydrodynamic response does not need more structural parameters, thus in order to simplify the design, the internal cross beams and other frame structures of this platform are not considered. Instead, an appropriate amount of outer plate thickness is given to replace it, as Tabs. 1b.

Table 1. The semi-submersible OC4 floating platform properties (Robertson et al., 2014).

(a) Geometry properties.

Depth of platform base below SWL (total draft)	20 m
Elevation of main column (tower base) above SWL	10 m
Elevation of offset columns above SWL	12 m
Spacing between offset columns	50 m
Length of upper columns	26 m
Length of base columns	6 m
Depth to top of base columns below SWL	14 m
Diameter of main column	6.5 m
Diameter of offset (upper) columns	12 m
Diameter of base columns	24 m
Diameter of pontoons and cross braces	1.6 m

(b) The wall thickness of each component.

Components	Main Column	Upper Column	Base Column	Pontoon
Wall Thickness	0.03 m	0.06 m	0.06 m	0.0175 m

From the Tabs.1, the whole OC4 platform could be construct. In this design of this platform, the density of wall steel plate is 7850 kg/m^3, so the metal of the structure is 3.8522E+6 kg. Considering to support the wind turbine including the tower, rotor and nacelle and balance the buoyancy, the offset columns are filled with ballast water, i.e. each upper column and base column. Ignoring the water moving or sloshing, the height of

ballast water in upper columns h_{wuc} is 7.83 m, and the height in base columns h_{wbc} is equal to 5.1078 m, as Fig. 4. The water density is 1025 kg/m^3, so the total water mass is 9.6208E+6 kg. All the structural of platform and ballast properties are listed in the Tab. 2.

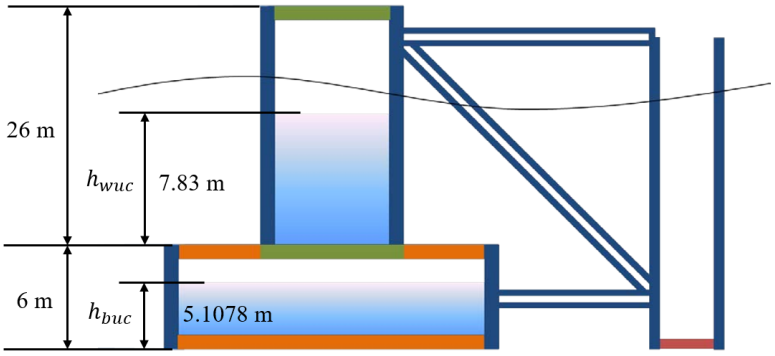

Figure 3. The ballast water filled in the offset column (Robertson et al., 2014).

Table 2. OC4 structural properties.

Light mass	3.85218E+6 kg
CoM location bellow SWL without ballast water	-8.6588 m
Roll inertia about CoM without ballast (Ixx)	2.56193E+9 kg·m^2
Pitch inertia about CoM without ballast (Iyy)	2.56193E+9 kg·m^2
Yaw inertia about CoM without ballast (Iyy)	4.24260E+9 kg·m^2
Ballast water mass	9.62080E+6 kg
Platform mass, including ballast	1.3473E+7 kg
CoM location bellow SWL, including ballast	-13.46 m
Moment inertia about CoM, including ballast (Ixx, Iyy, Izz)	(6.827E+9, 6.827E+9, 1.226E+10) kg·m^2

In addition, the effect of supper structure equipment such as wind turbine tower, rotor and nacelle to the total mass and moment inertia must be considered. Therefore, the mass distribution of each component and the total properties of OC4 floating offshore wind turbine platform are listed in the Tab. 3. The total mass is 14075746 kg, and the CoM is about 9.89 m bellow the surface waterline (SWL).

Table 3. Total mass and CoM location including the wind turbine.

	Mass	CoM location
Rotor	1.1E5 kg	89.35 m
Nacelle	2.4E5 kg	89.35 m
Tower	2.49718E+5 kg	43.4 m
OC4 platform	1.34730E+7 kg	-13.46 m
Total	1.4075746E+7 kg	-9.89 m

Thus, the moment inertia of the total platform is 1.071E+10 kg·m^2, 1.071E+10 kg·m^2 and 1.226E+10 kg·m^2 which represent the roll, pitch, yaw respectively.

3.2 Modifications of the Original OC4 Platform

In this paper, the inclined angle of upper columns is modified to 10 degrees and 20 degrees. The height of ballast water h_{wuc} and h_{wbc} in each column are adjusted to ensure the CoM of floating platform after installation of superstructure equipment. In addition, the ballast water in three upper columns also has been rotated due to the tank rotation. In the model with 10° incline, the vertical height h_{wuc} = 7.553 m, h_{wbc} = 5.172 m. While, in the model with 20° incline, the h_{wuc} = 7.174 m, and h_{wbc} = 5.286 m. Fig. 5 shows the geometric modeling with ballast water and mooring characteristics of the platform at prototype and inclined angle at 10° and 20°. The Tab. 4 lists the total structural properties after modification.

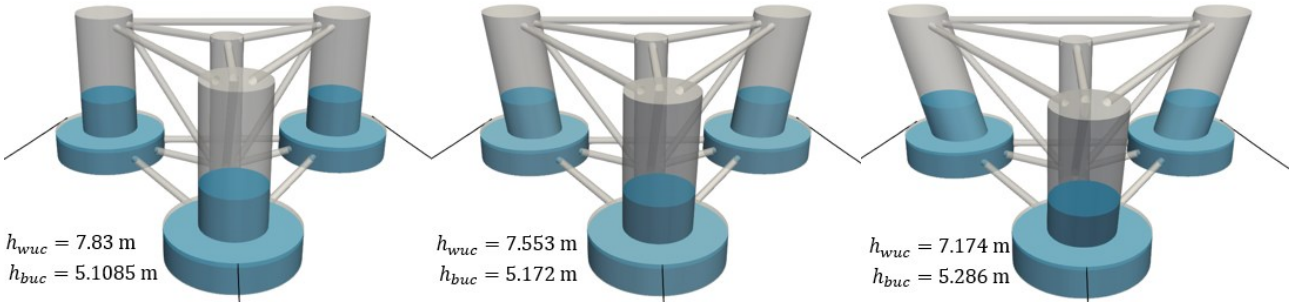

(a) Original OC4 platform (b) 10° inclined angle model (c) 20° inclined angle model

Figure 5. Geometric modeling and ballast water layout.

Table 4. Structural properties of the platform with inclined column.

(a) Only platform with ballast water.

	10° inclined angle model	20° inclined angle model
Light mass	3.92165E+6 kg	4.02628E+6 kg
Ballast water mass	9.65428E+6 kg	9.79968E+6 kg
CoM location bellow SWL, including ballast	-13.41 m	-13.34 m
Roll inertia about CoM, including ballast	7.0626E+9 kg·m^2	7.4689E+9 kg·m^2
Pitch inertia about CoM, including ballast	7.0626E+9 kg·m^2	7.4689E+9 kg·m^2
Yaw inertia about CoM, including ballast	1.2775E+10 kg·m^2	1.3551E+10 kg·m^2

(b) With NREL 5MW wind turbine.

	10° inclined angle model	20° inclined angle model
Total mass	1.4175E+7 kg	1.4425E+7 kg
Total CoM location	-9.89 m	-9.89 m
Roll inertia about CoM	1.1388E+10 kg·m^2	1.1791E+10 kg·m^2
Pitch inertia about CoM	1.1388E+10 kg·m^2	1.1791E+10 kg·m^2
Pitch inertia about CoM	1.2775E+10 kg·m^2	1.3551E+10 kg·m^2

3.3 Initial Mooring Setup

The positions of mooring points and anchor points have not changed which are listed in the Tab. 5 and shown in Fig. 5. The initial total mooring tension of each cable is approximately 1.097E+6 N, and 6.25 E+5 N on the z-direction.

Table 5. Mooring system properties (Robertson et al., 2014).

Depth to anchors below SWL	200 m
Depth to fairleads below SWL	14 m
Radius to anchors from platform centerline	837.6 m
Radius to fairleads from platform centerline	40.868 m
Unstretched mooring line length	835.5 m
Mooring line diameter	0.0766 m
Equivalent mooring line mass density	113.35 kg/m
Equivalent mooring line mass in water	108.63 kg/m
Equivalent mooring line extensional stiffness	753.6 MN
Hydrodynamic drag coefficient for mooring lines	1.1
Seabed drag coefficient for mooring lines	1.0

3.4 Simulation Domain and Grid Distribution

It is the most important for finite volume calculation method to draw a great grid distribution in the computational domain. The entire domain is set as 800 (x) × 480(y) × 260(z), as shown in Fig. 6. The center of main column is set at the (0, 0) in the domain, which means the CoM coordinates of the platform are (0, 0, -9.89) in the earth-fixed coordinate system. The inlet boundary is located at x = -300m, and the outlet boundary is located at the x = 500m. The length of sponge layer is 150 m, which is equal to one wave length λ. The boundary on both sides is a symmetrical plane, distributed on the both sides of the platform symmetrically.

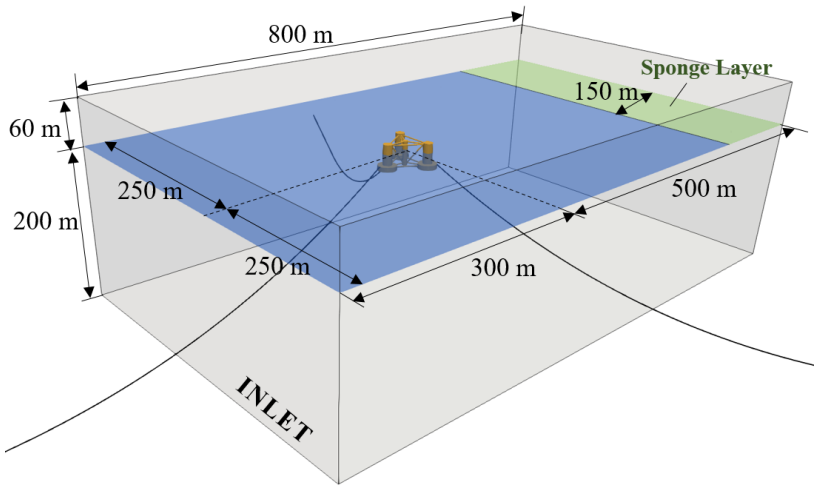

Figure 6. Simulation domain.

The second level of mesh refinement is used at free surface in order to guarantee the accuracy of calculation and the wave generation without attenuation. Thus, in the z-direction, a wave height range contains at least 15 grids, while in the x-direction, a wavelength range contains a least 80 grids. At the same time, set gradient changes in the x direction to ensure a denser mesh near the object. The main columns and offset columns adopt the third level encryption strategy, and the pontoons adopt fourth. Therefore, the total number of mesh grids for the original and inclined structures is approximately 2.98 million to 3.02 million. The Fig. 7 shows the mesh gird of simulation domain and platform structure.

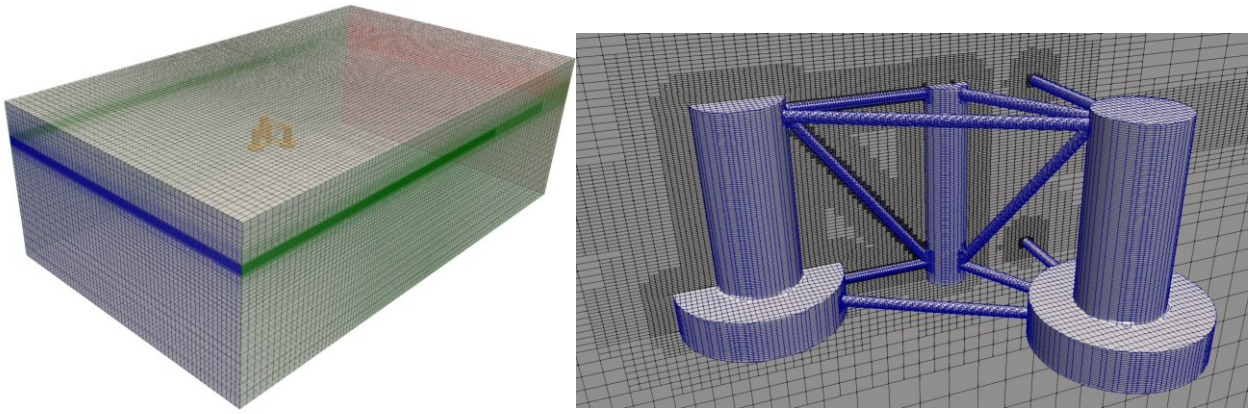

Figure 7. Mesh grid distribution.

4. RESULTS

4.1 Calculation Condition and Validation

In this research, a regular wave generated by Eqs. 7 and 8 are applied. The wave height is 7.58m, and the period is 9.80s, the wave length λ = 150m, as listed in Tab. 7

Table 7. Wave condition.

Wave height	Wave period	Wave length
7.58 m	9.80 s	150 m

There are three points (x = -200m, 0m, 450m) in the simulation domain to monitor the wave elevation in an empty tank. Among these, the wave gauge at x = 450m is used to validate the absorption zone effect. All of the results are shown in Fig. 8, compared with the theoretical data.

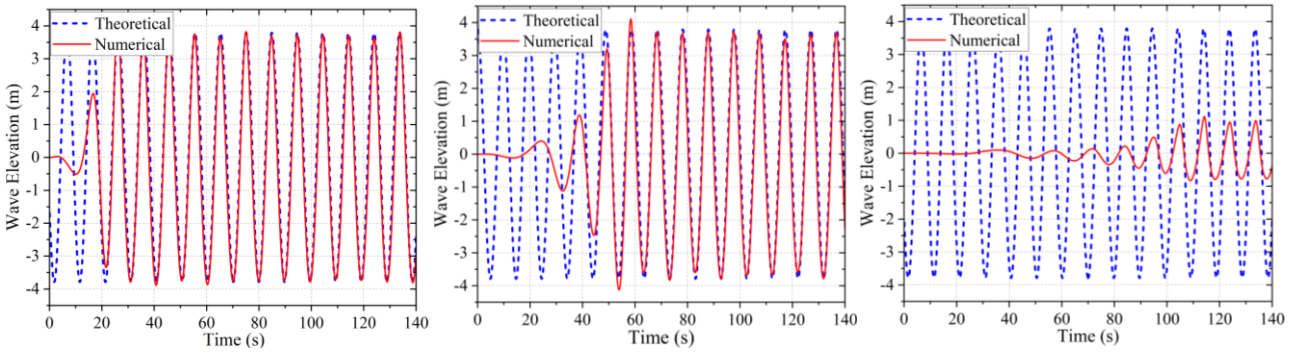

(a) x = -200 m (b) x = 0 m (c) x = 450 m

Figure 8. Wave elevation for the wave gauges.

The figures indicate that the wave generated by naoe-FOAM-SJTU could agree well with the theoretical data. Besides, the damping zone have a good significant to attenuate the waves. Therefore, the wave generation and absorbing module for naoe-FOAM-SJTU solver utilized in this paper is accurate and reliable.

4.2 Motion Response

The motion response of three different platforms is shown in Fig. 9. Only surge, heave and pitch three DOFs change apparently due to the wave propagation direction along the x-axis. From the figure, it indicates that as the increase of inclined angle, the stable position of surge motion and the amplitude of heave motion increased gradually. The reason for increasement of both can be attributed to the wetted area expanding near the free surface, which could provide more hydrodynamic forces obtained from the wave energy. However, the pitch motion shows a decreasing trend. It is mainly contributed by the increasement of moment inertia.

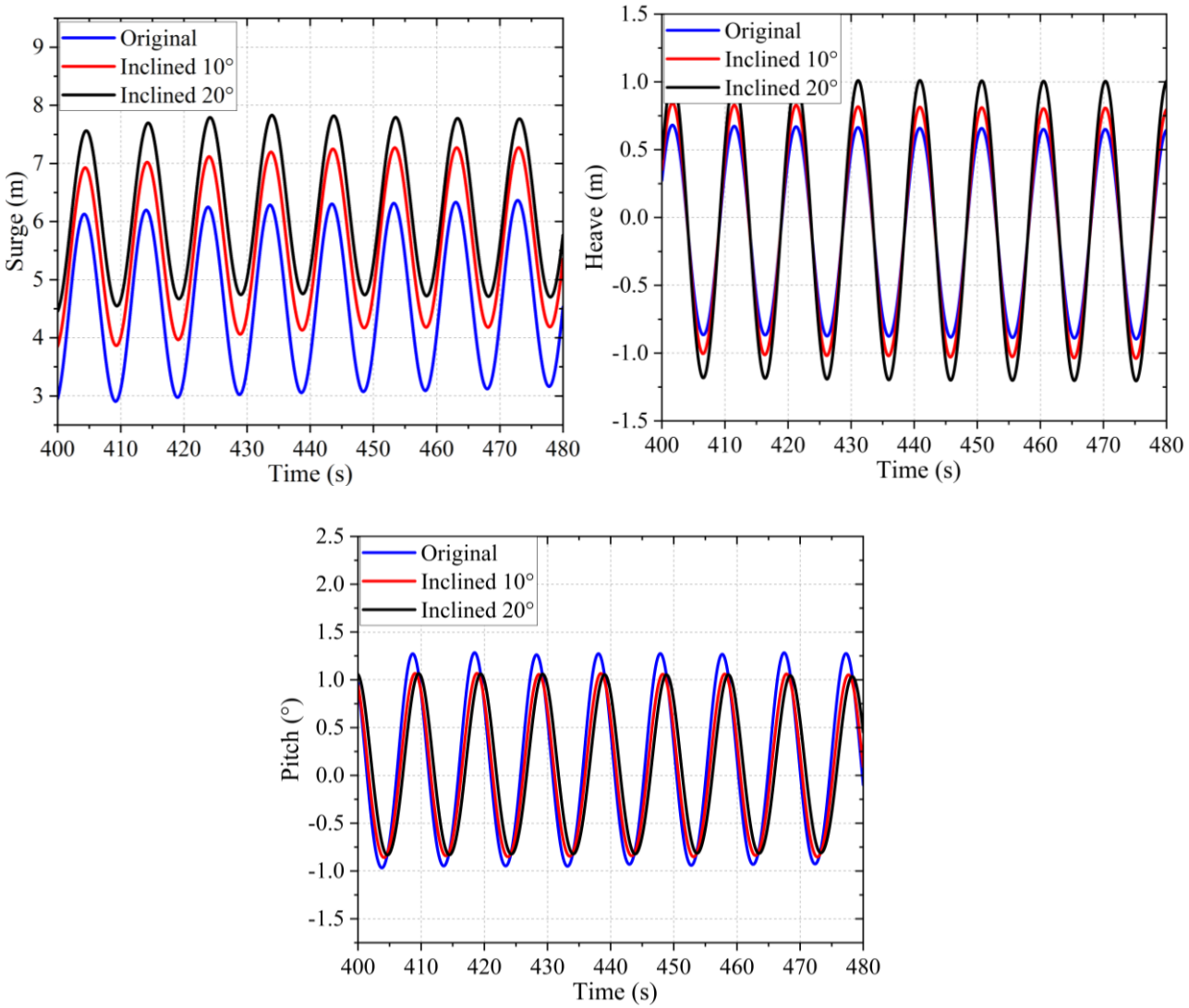

Figure 9. Wave elevation for the wave gauges.

Through the statistical analysis of the data, we found that the surge motion of different platforms remained stable within ±1.54 m, which is also the amplitude. The stable position of original OC4 platform is at 4.71 m, the inclined 10° model is at x = 5.72 m, and the inclined 20° model is at x = 6.25 m. For heave motion, the stable position for these three models is z = -0.1185 m, z = -0.113 m, z = -0.0985 m. And the amplitude for

those these is 0.769 m , 0.918 m, 1.1035 m respectively. Compared with the original, the inclined 10° model increase 19.38 %, and inclined 20° model increase 43.50 %. And the amplitude for pitch motion is 1.105°, 0.955°, 0.933° respectively.

4.3 Hydrodynamic Response

Due to the ability of CFD to provide complete hydrodynamic data, the wave surface elevation and platform dynamic pressure color map when the front column is located at the peak position has been shown in Fig. 10.

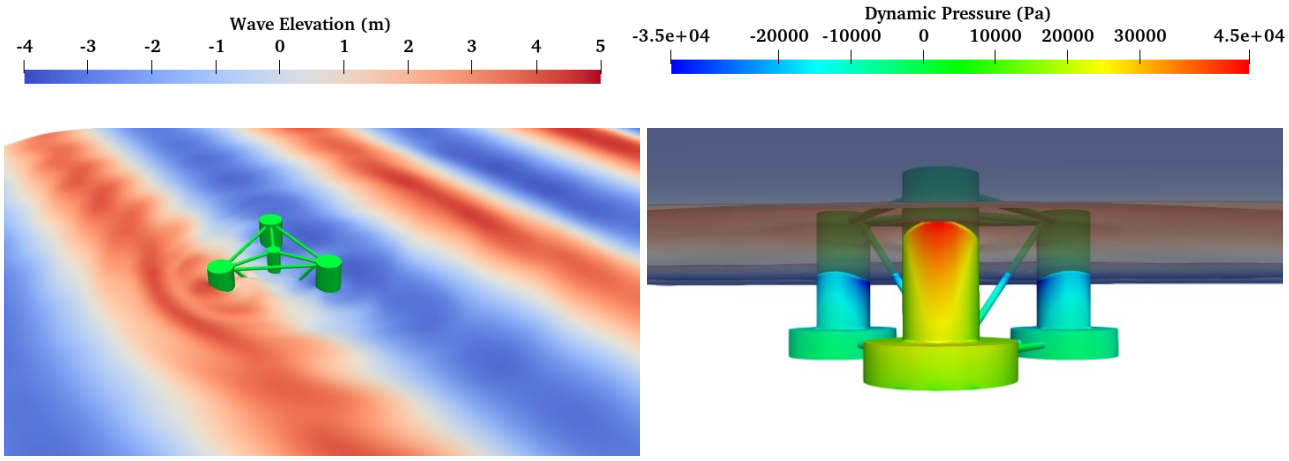

(a) Original OC4 platform

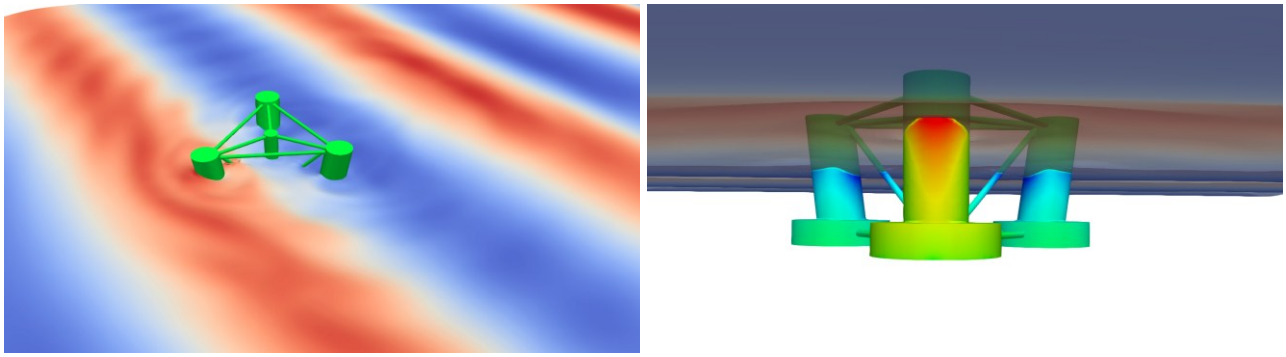

(b) 10° inclined angle model

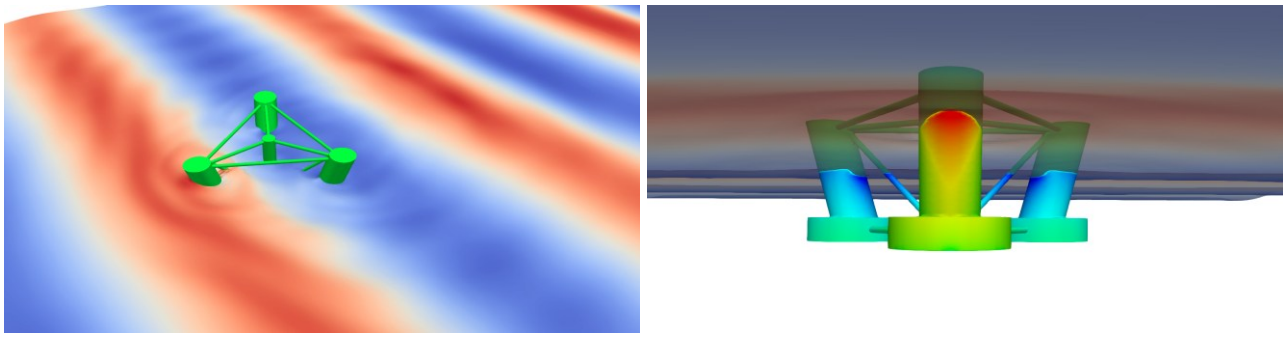

(c) 20° inclined angle model

Figure 10. Wave elevation and dynamic pressure.

5. CONCLUAISON

In this article, by modifying the inclination angle of the offset columns for OC4 FOWT platform and the motion and dynamic response of the platform under regular wave is studied based on CFD method. It was found that as the tilt angle increases, the platform's surge stable position shifts towards the positive x-axis direction, resulting in an increase in the amplitude of heave motion and a decrease in the amplitude of pitch motion. Compared to the original model, the heave motion amplitude for inclined 10 degrees and 20 degrees angle the amplitude increases 19.38 % and 43.50%, and the pitch motion amplitude decreases 13.57% and 15.57%. In the research of floating offshore wind turbine, the harm of pitch motion to the wind turbine is enormous. It has more engineering significance to sacrifice the heave motion for reducing the pitch by modifying the inclined angle.

ACKNOWLEDGEMENTS

This work was supported by the National Natural Science Foundation of China (52131102), and the National Key Research and Development Program of China (2019YFB1704200), to which the authors are most grateful.

REFERENCES

Bagbanci, H., Karmakar, D., and Guedes Soares, C. (2012). Review of offshore floating wind turbines concepts. Maritime Engineering and Technology, 553-562.

Brommundt, M., Krause, L., Merz, K., and Muskulus, M. (2012). Mooring System Optimization for Floating Wind Turbines using Frequency Domain Analysis. Energy Procedia, 24, 289-296.

Cheng, P., Huang, Y., and Wan, D. C. (2019). A numerical model for fully coupled aero-hydrodynamic analysis of floating offshore wind turbine. Ocean Engineering, 173, 183-196.

Coulling, A. J., Goupee, A. J., Robertson, A. N., Jonkman, J. M., and Dagher, H. J. (2013). Validation of a FAST semi-submersible floating wind turbine numerical model with DeepCwind test data. Journal of Renewable and Sustainable Energy, 5(2).

Ferri, G., Marino, E., and Borri, C. (2020). Optimal Dimensions of a Semisubmersible Floating Platform for a 10 MW Wind Turbine. Energies, 13(12), 3092.

Ferri, G., Marino, E., Bruschi, N., and Borri, C. (2022). Platform and mooring system optimization of a 10 MW semisubmersible offshore wind turbine. Renewable Energy, 182, 1152-1170.

Global Wind Energy Council (2022). Global wind report 2022. Global Wind Energy Council Brussels, Belgium.

Karimi, M., Hall, M., Buckham, B., and Crawford, C. (2017). A multi-objective design optimization approach for floating offshore wind turbine support structures. Journal of Ocean Engineering and Marine Energy, 3(1), 69-87.

Liu, Z., Zhou, Q., Tu, Y., Wang, W., and Hua, X. (2019). Proposal of a Novel Semi-Submersible Floating Wind Turbine Platform Composed of Inclined Columns and Multi-Segmented Mooring Lines. Energies, 12(9), 1809.

Robertson, A., Jonkman, J., Masciola, M., Song, H., Goupee, A., Coulling, A., and Luan, C. (2014). Definition of the Semisubmersible Floating System for Phase II of OC4 (NREL/TP-5000-60601). N. R. E. Laboratory.

Sclavounos, P., Tracy, C., and Lee, S. (2008). Floating Offshore Wind Turbines: Responses in a Seastate Pareto Optimal Designs and Economic Assessment. ASME 2008 27th International Conference on Offshore Mechanics and Arctic Engineering,

Tran, T. T., and Kim, D.-H. (2015). The coupled dynamic response computation for a semi-submersible platform of floating offshore wind turbine. Journal of Wind Engineering and Industrial Aerodynamics, 147, 104-119.

Wang, J.-h., Zhao, W.-w., and Wan, D.-c. (2019). Development of naoe-FOAM-SJTU solver based on OpenFOAM for marine hydrodynamics. Journal of Hydrodynamics, 31(1), 1-20.

Xu, S., Xue, Y., Zhao, W., and Wan, D. (2022). A Review of High-Fidelity Computational Fluid Dynamics for Floating Offshore Wind Turbines. Journal of Marine Science and Engineering, 10(10), 1357.

Xu, S., Zhuang, T., Zhao, W., and Wan, D. (2023). Numerical investigation of aerodynamic responses and wake characteristics of a floating offshore wind turbine under atmospheric boundary layer inflows. Ocean Engineering, 279, 114527.

Zhang, H., Wang, H., Cai, X., Xie, J., Wang, Y., and Zhang, N. (2022). Research on the Dynamic Performance of a Novel Floating Offshore Wind Turbine Considering the Fully-Coupled-Effect of the System. Journal of Marine Science and Engineering, 10(3), 341.